PROCEEDINGS, 50th Workshop on Geothermal Reservoir Engineering
Stanford University, Stanford, California, February 10-12, 2025
SGP-TR-229

Assessing Stress and Fracture Distribution in Enhanced Geothermal Systems using Shear Wave Splitting Analysis at Utah FORGE

Jaewoo Kim, Jonathan Ajo-Franklin, and the FOGMORE@FORGE Team

Department of Earth, Environmental and Planetary Sciences, Rice University, 6100 Main St., Houston, TX 77005

jk103@rice.edu

Keywords: Utah FORGE, shear wave splitting, seismic anisotropy, microseismic monitoring, stress orientation, fracture network

ABSTRACT

Effective development of Enhanced Geothermal Systems (EGS) provide the potential for low CO_2 baseload energy by artificially creating permeability in hot low-permeability rocks, yet fluid injection can induce seismicity and alter local stress fields. At the Utah FORGE (Frontier Observatory for Research in Geothermal Energy) site, we investigate fracture and stress state variability through use of Shear Wave Splitting (SWS) analysis, employing the Eigenvalue method to measure fast shear wave polarization (ϕ) and delay time (δt). Using data from the FOAL 1 (FORGE Observation Array Linear) nodal experiment, we observe two distinct clusters in SWS parameters that suggest spatially varying fracture characteristics and stress regimes. Sensors located above the 16A well show higher δt values and NNE-SSW direction of ϕ, indicative of increased fluid-filled fracture. Meanwhile, sensors located on the east side of end of 16A well show explicitly lower δt values and NNW-SSE direction of ϕ, which suggest different fluid-filled crack structures that could originate from a pre-existing fault. These findings highlight SWS as a valuable tool for detecting changes in fracture networks and stress states, ultimately providing insights for more effective reservoir management.

1. INTRODUCTION

1.1 Geothermal energy and induced seismicity

Geothermal energy plays a crucial role in meeting evolving global energy needs, providing a renewable, reliable, and continuous alternative to traditional sources like coal and nuclear power, which are increasingly challenged by environmental concerns. Geothermal energy enhances energy security, sustainability, and the transition to a cleaner energy future by complementing intermittent renewables like solar and wind. In particular, Enhanced Geothermal Systems (EGS), which create artificial permeability to enable fluid circulation, have seen rapid expansion over the past five years due to the adoption of hydraulic fracturing techniques from the oil and gas sector. This advancement has allowed commercial-scale geothermal production even in low-permeability rocks.

However, fluid injection or extraction in the subsurface, such as in hydraulic fracturing for shale gas (Schultz et al., 2020), CO_2 sequestration (Cheng et al., 2023), EGS (Kim et al., 2018), and natural gas production (van Thienen-Visser and Breunese, 2015) can induce seismicity. The importance of seismic monitoring is underscored by the implementation of traffic light systems (Baisch et al., 2019), which mandate the suspension of operations if induced seismicity exceeds certain thresholds. This is particularly critical for commercial-scale EGS sites (Kim et al., 2018), where the ability to provide stable, uninterrupted energy—unlike other renewable sources—can be compromised if the risks associated with induced seismicity are not effectively managed.

Injection-induced seismicity primarily occurs due to the increase in pore pressure during the injection process, which reduces the effective normal stress and facilitates shear slip along faults. When this process occurs on pre-existing faults, it can trigger larger magnitude seismic events (e.g. Kim et al., 2018). Therefore, monitoring the subsurface stress distribution through seismological approaches can provide crucial insights into managing these risks.

1.2 Shear wave splitting and seismic anisotropy

Seismic anisotropy offers a valuable tool for understanding the stress state of a site in such contexts. One manifestation of seismic anisotropy is shear wave splitting (SWS), a phenomenon where a shear wave splits into two orthogonal components—a 'fast' and a 'slow' shear wave—due to differences in their velocities. This occurs when the shear wave traverses an anisotropic medium. SWS can be quantified by two parameters: the polarization direction of the fast shear wave (ϕ) and the time delay (δt) between the fast and slow shear waves (Crampin, 1978). Crustal anisotropy is generally caused by (i) aligned fluid-filled micro-cracks (stress-induced anisotropy) or (ii) macroscopic structural properties (structure-induced anisotropy), such as fractures or faults (Boness and Zoback, 2006). Stress-induced anisotropy arises from fluid-filled microcracks aligned with the maximum horizontal stress (Crampin and Peacock, 2008). Microcracks not aligned with this stress are 'closed,' redirecting fluids into 'open' cracks aligned with the maximum horizontal stress, causing the fast shear wave to polarize parallel to these open cracks, while the orthogonally polarized wave travels more slowly. On the other hand, structure-induced anisotropy often results from crystal-preferred orientations parallel to macroscopic features such as pre-existing faults or folds (Licciardi et al., 2018). Since SWS is sensitive to fluid-filled microcracks, this tool can be used to monitor spatio-temporal changes of fluid process (Nolte et al., 2017; Kim and Kim 2022).

1.3 Utah FORGE (Frontier Observatory for Research in Geothermal Energy)

Due to the substantial research focus on enhanced geothermal systems (EGS), the FORGE site has become a key scientific test bed for technological advancements in EGS, supported by the U.S. Department of Energy and managed by the University of Utah. Located about 350 km south of Salt Lake City near Milford, Utah, the site is situated on the western flank of the Mineral Mountains, on an alluvial fan west of the Opal Mound Fault and the Roosevelt Hot Spring hydrothermal system. The Utah FORGE site lies atop recent alluvial sediments and tuffs down to approximately 1 km, beneath which lay granitoid bedrock, with the basement contact dipping westward at angles between 20 to 35 degrees. This contact's depth and topography are crucial for planning future EGS wells, particularly towards the basin's axis, where deeper sediment cover exists. Current information on this contact comes from a previously conducted seismic reflection survey (Moore et al., 2019) and logs from existing wells. Data on lithology and mineralogy are primarily obtained from the Utah FORGE injection well, 16A(78)-32, which extends vertically to a depth of 2,000 meters before deviating eastward to a depth of 2,500 meters. Well 58-32, located about 700 meters east of well 16A, extends vertically to a depth of approximately 2,300 meters. The Utah FORGE project has a continuous seismic monitoring system utilizing multiple wells. Well 16B(78)-32, nearly parallel to 16A(78)-32, has a DAS fiber extending to a depth of 2,500 meters near the well's toe. A geophone and an accelerometer are permanently installed at the bottom of well 68-32. Additionally, vertical borehole DAS systems have been installed in two vertical seismic monitoring wells, 78A-32 and 78B-32.

The FOAL 1 (FORGE Observation Array Linear) experiment, conducted in the spring of 2022, was specifically designed to densely sample and capture direct and converted P and S waves generated by microseismic events during EGS stimulation activities (Kim et al., 2023). The array consisted of 100 3- component 5Hz geophones (Smart Solo IGU 16HR-3C), arranged to follow the trajectory of well 78-16A and align parallel to the slope direction of the granite interface (Figure 1). The geophones were buried at a depth of about 7 cm, starting from the west of well 16A and extending to the Opal Mound Fault, with a spacing of approximately 35 m, except for the gap near the pad of well 16A. The node locations were surveyed using sub-meter DGPS (with 25 cm accuracy), and a digital compass was employed for component alignment. The FOAL 2 experiment, conducted in April of 2024, expanded this geometry into a 2-dimensional array with multiple lines of sensors, incorporating the 100 geophones from FOAL 1 along with 700 single-component geophones (STRYDE). This expansion was designed for multiple imaging and monitoring approaches, including moment tensor inversion and ambient noise tomography.

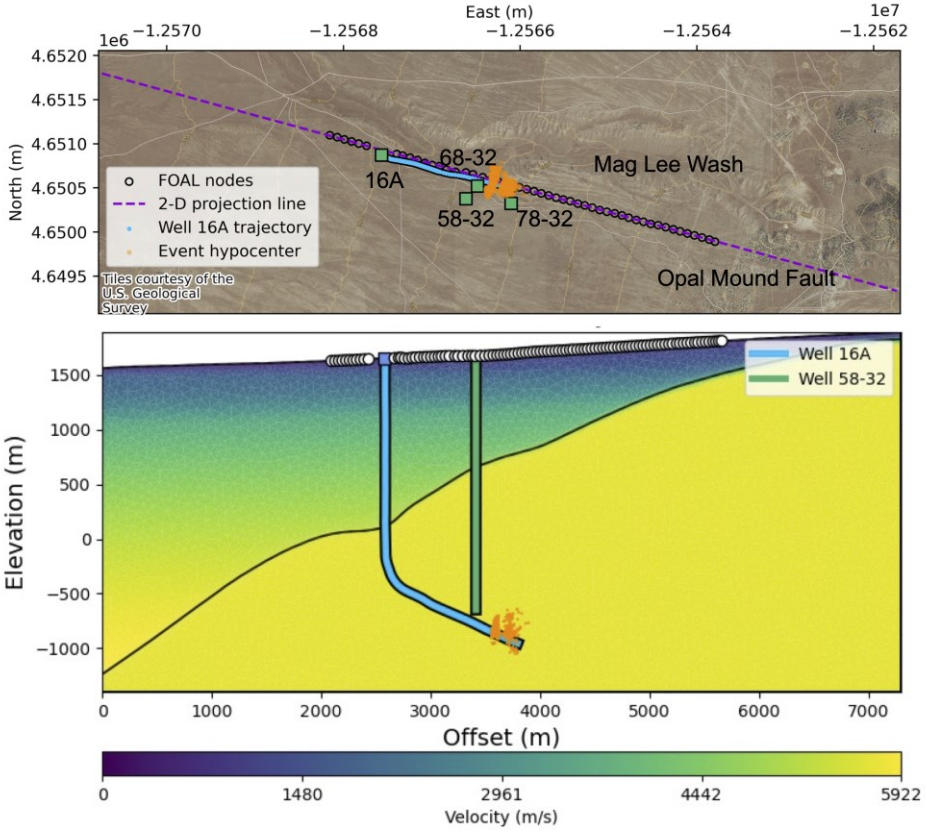

Figure 1: (a) FOAL 1 acquisition geometry with nearby well (green square) and major geological structures on surface (b) Cross-section constructed in alignment with the FOAL 1 nodes. Note that each well is projected and superimposed. The seismicity depicted in this figure represents the observed events during the stimulation period from April 16th to April 22nd, 2022 as reported by Geo-Energie-Suisse (Dyer et al., 2022).

1.4 Review of seismic anisotropy studies at the Utah FORGE site

Several studies have reported on seismic anisotropy at the Utah FORGE site or on FORGE core samples. The first study by Li et al. (2024) focused on the time-lapse variations in Shear-wave Splitting Rates (SSR) observed during induced microearthquakes from Phase 2C fracture stimulations at the site. The data discussed in that study were recorded between April 19 and May 3, 2019, using a downhole seismic observation system installed in the monitoring well 78-32. This system was comprised of twelve three-component (3C) geophones deployed at depths ranging from 645 to 980 meters and a DAS fiber-optic cable. The study identified a significant increase in SSR over time, which was linked to the increasing heterogeneity and fracturing within the granitic rocks as a result of the ongoing stimulation stages. The second study by Carrasquilla et al. (2024) focused on laboratory measurements of seismic anisotropy in granitic core samples from well 58-32. The study revealed that both P-wave and S-wave anisotropy decreased with increasing confining pressure. These results suggest that an increase in pore fluid pressure during EGS hydraulic fracturing could lead to an increase in seismic anisotropy while effective pressure decreases, highlighting the dynamic relationship between pressure conditions and anisotropy in the reservoir. A third study worth mentioning by Xing et al. (2022) was not directly related to seismic anisotropy but examined in-situ stress measurements at the FORGE site, highlighting the NNE-SSW orientation of the maximum horizontal stress (SHmax). Xing et al.'s consistent stress orientation was inferred from the azimuths of induced fractures observed in Formation MicroScanner Image (FMI) logs. The study emphasized the importance of understanding stress orientation and its response to hydraulic stimulation for optimizing fracture development in geothermal reservoirs.

2. SHEAR WAVE SPLITTING MEASUREMENT

We will employ the Eigenvalue method (Silver and Chan, 1991) for measuring SWS parameters. This semi-automatic technique is widely used for SWS measurements because it reduces user bias compared to manually picking the orientation of the initially arriving fast shear wave. In Silver and Chan (1991), the splitting operator $\Gamma(\phi, \delta t)$ is used to produce the split waveform u as u_s:

$$\boldsymbol{u_s(\omega) = u(\omega)\,\Gamma(\phi, \delta t)\cdot n} \tag{1}$$

where $u(\omega)$ is the displacement function of the initial shear wave and n is the ray propagation unit vector. The splitting operator is defined as:

$$\boldsymbol{\Gamma(\phi, \delta t) = e^{-\frac{i\omega\delta t}{2}}\hat{f}\hat{f}^T + e^{-\frac{i\omega\delta t}{2}}\hat{s}\hat{s}^T} \tag{2}$$

where $\hat{f}$ and $\hat{s}$ are fast and slow shear wave vectors. To determine the correct SWS parameters (ϕ, δt), we perform a grid search by applying various inverse splitting operators (Γ^{-1}) to the observed waveform until the wave is linearized, as assumed. The linearity of the corrected shear wave is quantified by computing the eigenvalues of a two-dimensional time domain covariance matrix. The covariance matrix between two perpendicular horizontal components (i and j) for any given pair of ϕ and δt is determined as:

$$\boldsymbol{C_{ij}(\phi, \delta t) = \int_{-\infty}^{\infty} u_i(t)u_j(t-\delta t)\,dt} \tag{3}$$

For an ideally linear wave, the covariance matrix will have a single non-zero first eigenvalue (λ_1) while second eigenvalue (λ_2) will be zero. Therefore, the Eigenvalue method involves conducting a grid search for SWS parameters that yield the most linearized corrected waveform, in other words, the parameters that minimize the second eigenvalue of the covariance matrix within the selected time window.

Seismic data for this study were obtained from the FOAL 1 array, which, as mentioned previously, includes 100 three component geophones deployed near the surface along the trajectory of the 16A well (Figure 1). During the deployment period in April 2022, we created a preliminary catalog using a multi-channel STA/LTA (Short Term Average/Long Term Average) event detection method. This method was used in conjunction with a reference catalog provided by Geo-Energie-Suisse (GES), which was based on data from a borehole geophone array. We applied a bandpass filter ranging from 10 to 50 Hz and used a 0.5-second STA window and a 10-second LTA window, with triggering thresholds of 2.5 and 2.0, respectively. An event was considered detected if it triggered on more than 40 geophones. Using this STA/LTA method, we detected a total of 13 events, four of which were not reported in the original GES catalog. Including 8 additional earthquakes from the GES catalog, a total of 21 events were used in our analysis.

For each event-station pair, we conducted SWS measurements using a 2-second time window around the S-wave arrival. A grid search was performed to find the optimal δt and ϕ. The search was conducted for δt within a range of 60 ms at 2 ms intervals, and for ϕ across all directions in azimuth with a spacing of 0.1 degrees. To ensure data quality, we applied several filtering criteria. First, we discarded data where the maximum amplitude of the vertical component exceeded that of the horizontal components, as this indicated a distorted S-wave due to a lower incidence angle (Savage et al., 2016). Second, we computed the second eigenvalue of the covariance matrix from the observed horizontal components and filtered out data with a second eigenvalue less than 1.5, which suggests that the waveform was not split. Finally, we visually inspected the map of second eigenvalues (Figure 3), waveforms, and particle motion to grade the overall measurement quality (A, B, C). Only measurements with A and B grades were used for interpretation.

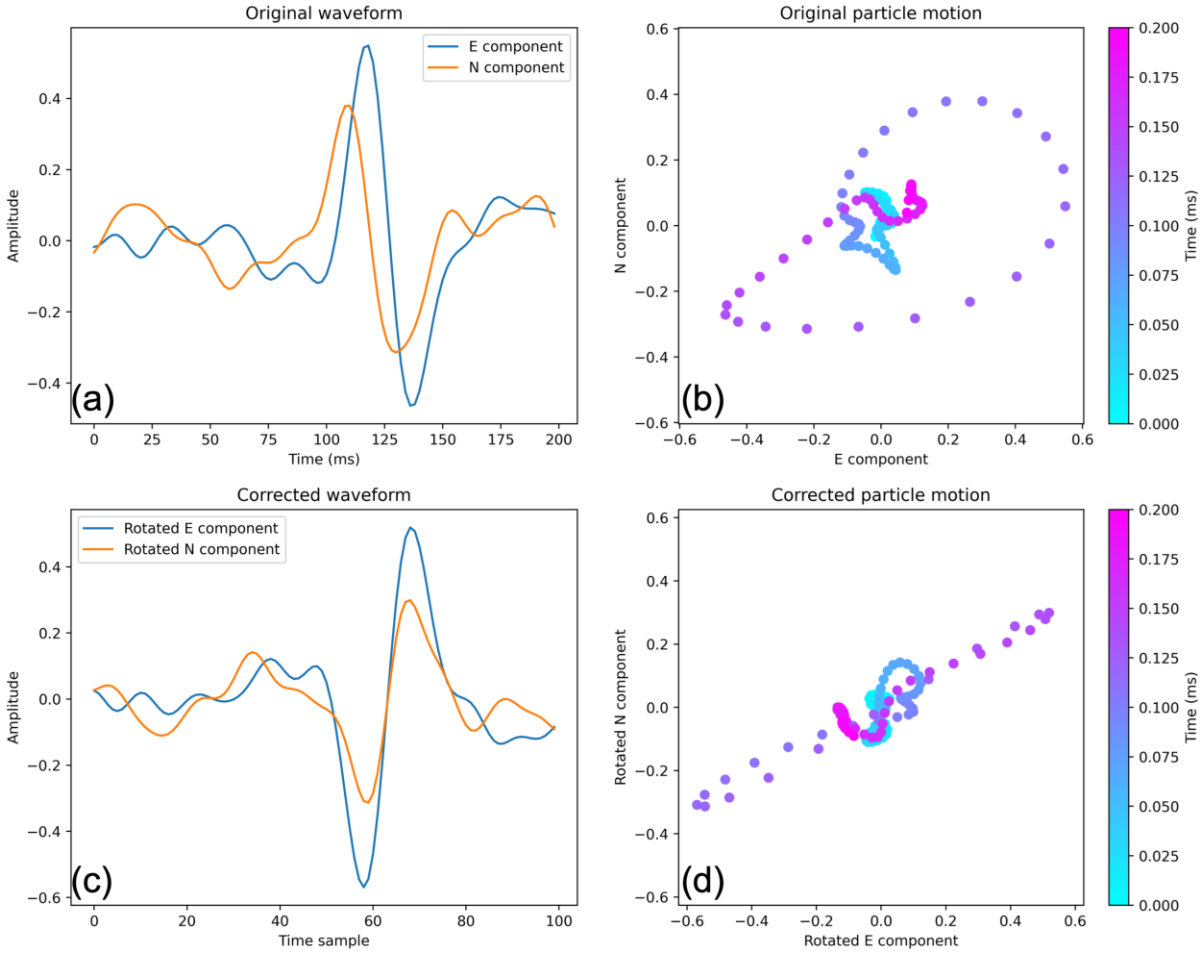

Figure 2: Example of grade 'A' SWS measurement. (a) Original waveforms for the E (East) and N (North) components of the S-wave arrival before correction. (b) Particle motion for the original waveform, showing elliptical polarization indicative of shear-wave splitting. (c) Corrected waveforms after applying the inverse splitting operator, resulting in linearized shear waveforms for the rotated E and N components. (d) Corrected particle motion, demonstrating linear polarization after shear-wave splitting correction, indicating successful SWS analysis.

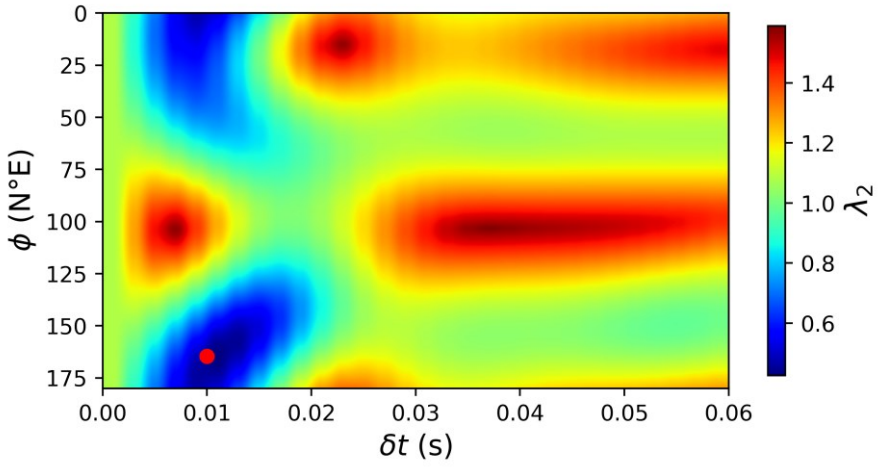

Figure 3: Eigenvalue map of the second eigenvalue (λ2) for the previously mentioned SWS analysis case (Figure 2). The map shows λ2 as a function of the fast shear wave orientation (ϕ) and delay time (δt), where lower values of λ2 (blue regions) indicate more linearized waveforms. The red dot marks the optimal SWS parameters with the minimum λ2, representing the best-fitting combination of ϕandδt that produces the most linearized corrected shear wave (Figure 2).

3. RESULTS

We obtained total 375 SWS measurements before grading. After grading, we identified 86 'A' grade and 50 'B' grade measurements, which represent good quality data. The overall results of ϕ shown in Figure 4, with the mean value of −12.8° ±34.5°. The discrepancy between our results and those of Li et al. (2024), as well as the relatively large standard deviation, can be attributed to the fact that our measurements fall into two distinct clusters. One cluster is oriented towards the NNW and the other towards the NNE, which contributes to the variation in the mean ϕ values. On the other hand, δt has 11.2 ± 5.7 ms for good quality measurement, and if we convert this value to SSR, it will be likely having around 0.7% which is slightly lower than percentage anisotropy measured from Li et al. (2024) that had ranged between 0.5% to 1.5%.

Upon closer inspection, we observed that the SWS parameters are divided into two distinct clusters. For δt, there is a clear difference between the sensors located above the 16A well trajectory (west sensors) and the remaining east sensors (Figure 6). The δt values for the west sensors were 17.7 ± 2.9 ms, while the east sensor group showed 8.9 ± 4.6ms, indicating a nearly twofold difference. Similarly, for ϕ, the west group exhibited a NNE orientation with an average of +6.7° ± 18.7°, whereas the east group showed a NNW orientation with an average of −24.3° ± 35.3°.

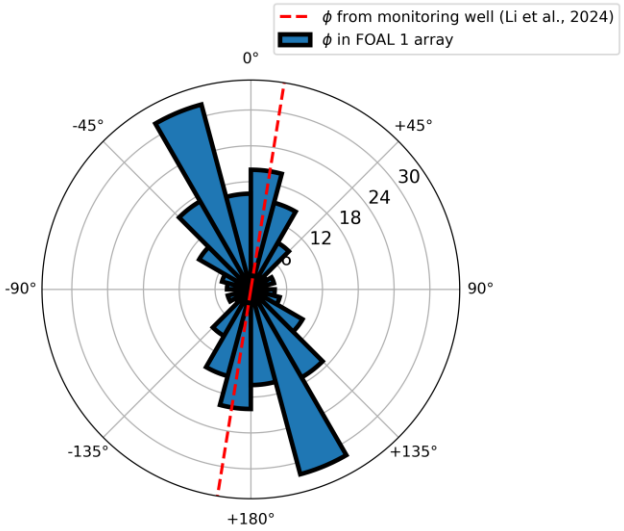

Figure 4: Comparison of fast shear wave orientations (ϕ) between the FOAL 1 array (solid blue bars) and the monitoring well data from Li et al. (2024) (dashed red line). The rose diagram displays the distribution of ϕ measurements across the FOAL 1 array, using high-quality data (grades 'A' and 'B'). The red dashed line indicates the fast shear wave orientation derived from the monitoring well, showing general agreement with the orientations observed in the FOAL 1 array.

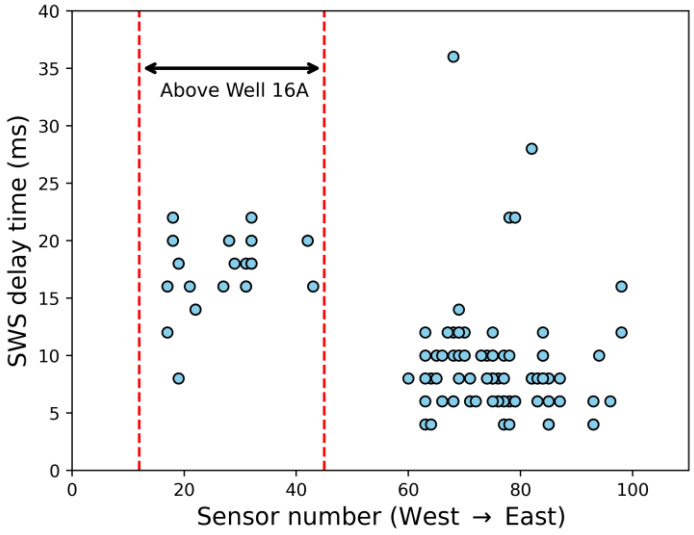

Figure 5: SWS delay times as a function of sensor number from the FOAL array. The sensors between indices 12 and 45 (highlighted by red dashed lines) are located directly above the L-shaped trajectory of Well 16A, which runs beneath the surface.

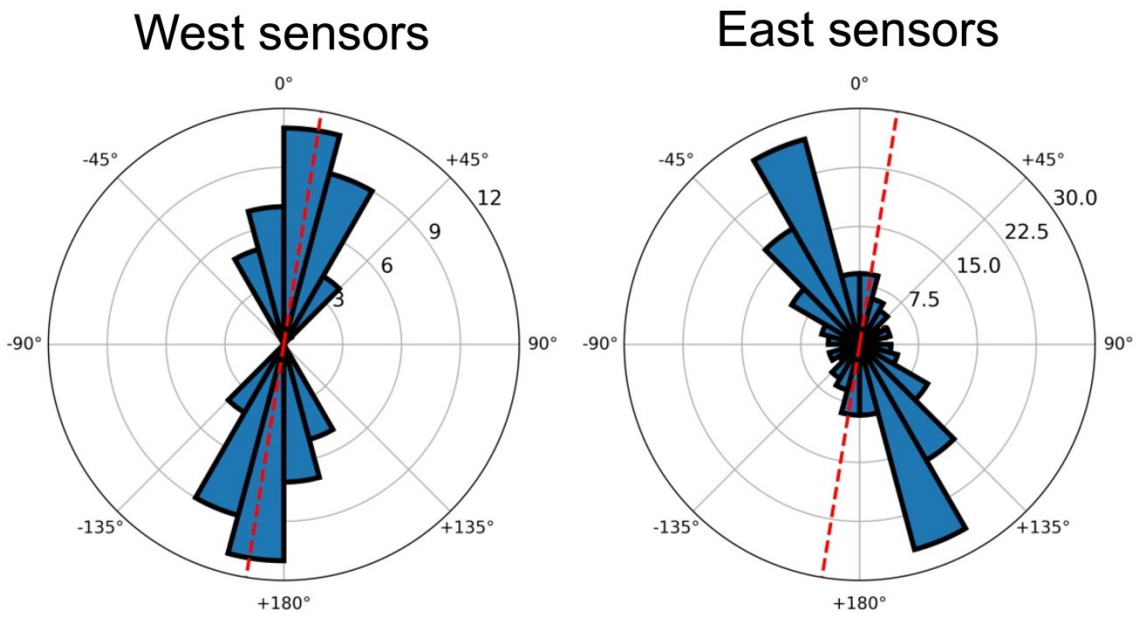

Figure 6: Rose diagrams showing the distribution of fast shear wave orientation in the FOAL 1 array, divided into two groups: (a) West sensors located above the 16A well trajectory and (b) East sensors.

4. DISCUSSION AND CONCLUSION

Our analysis of SWS parameters from the FOAL 1 array reveals significant spatial variability in seismic anisotropy and subsurface stress at the Utah FORGE site. Sensors above the 16A well trajectory exhibited stronger shear wave splitting, indicated by higher delay times compared to the east sensors. This suggests that hydraulic stimulation near the well has led to increased micro-cracking and fluid migration in this region, impacting the local stress field.

The distinct clustering of fast shear wave orientations between the west and east sensor groups can be explained by two potential scenarios: (1) a varying stress regime across the site, or (2) geological structures that create directional anisotropy. In the first scenario, poroelastic stress modeling suggests that continuous fluid injection and fracture opening may have altered the local stress regime. In the second scenario, pre-existing geological structures, such as faults, may have induced anisotropy through crystal-preferred orientation aligned with the fault strike. However, these hypotheses remain speculative, as we have limited microseismic activity in the eastern part of the injection area, which restricts our ability to fully investigate these scenarios. If the SWS parameter variations do in fact indicate spatial and possibly temporal variations in stress state across the Utah FORGE site, such changes could significantly impact hydraulic fracture geometry and will be useful in modeling analysis of the April 2024 16A/16B stimulation activities.

Future studies could benefit from utilizing the FOAL 2 array, a two-dimensional surface array, to investigate fracture extension by observing changes in anisotropy along the north-south direction. Additionally, comparing the temporal evolution of anisotropic parameters between the FOAL 1 (2022) and FOAL 2 (2024) arrays could offer further insights into the dynamic evolution of the fracture network and stress field over time.

5. ACKNOWLEDGMENTS

The Utah FORGE site is supported by DOE EERE Geothermal Technologies Office oto Utah FORGE and the University of Utah under Project DE-EE0007080 Enhanced Geothermal System Concept Testing and Development at the Milford City, Utah. The authors thank to the FOGMORE@FORGE (Fiber Optic Geophysical Monitoring of Reservoir Evolution) team for their collaboration (Utah FORGE R&D Project 3-2417)

REFERENCES

Baisch, S., Koch, C., and Muntendam-Bos, A.: Traffic light systems: To what extent can induced seismicity be controlled?, Seismological Research Letters, 90, 1145–1154 (2019).

Boness, N. L., and Zoback, M. D.: Mapping stress and structurally controlled crustal shear velocity anisotropy in California, Geology, 34, 825–828 (2006).

Carrasquilla, M. D., Sun, M., Long, T., Sisson, V., Lapen, T., Jones, C., Moore, J., Huang, L., and Zheng, Y.: Seismic anisotropy of granitic rocks from a fracture stimulation well at Utah FORGE using ultrasonic measurements, Geothermics, 123, 103129 (2024).

Cheng, Y., Liu, W., Xu, T., Zhang, Y., Zhang, X., Xing, Y., Feng, B., and Xia, Y.: Seismicity induced by geological CO_2 storage: A review, Earth-Science Reviews, 239, 104369 (2023).

Crampin, S.: Seismic-wave propagation through a cracked solid: polarization as a possible dilatancy diagnostic, Geophysical Journal International, 53, 467–496 (1978).

Crampin, S., and Peacock, S.: A review of the current understanding of seismic shear-wave splitting in the Earth's crust and common fallacies in interpretation, Wave Motion, 45, 675–722 (2008).

Dyer, Ben, Karvounis, Dimitrios, & Bethmann, Falko. Utah FORGE: Updated Seismic Event Catalogue from the April, 2022 Stimulation of Well 16A(78)-32. United States. https://dx.doi.org/10.15121/1908927

Feng, Z., Huang, L., Chi, B., Gao, K., Li, J., Ajo-Franklin, J., Blankenship, D. A., Kneafsey, T. J., E. C. Team, et al.: Monitoring spatiotemporal evolution of fractures during hydraulic stimulations at the first EGS Collab testbed using anisotropic elastic-waveform inversion, Geothermics, 122, 103076 (2024).

Kim, J., Ajo-Franklin, J., Shadoan, T., Sobolevskaia, V., Correa, J., and Freifeld, B.: A dense linear array for passive seismic imaging of geothermal structural features: The FOAL experiment at Utah FORGE, Proceedings, Third International Meeting for Applied Geoscience & Energy, Society of Exploration Geophysicists and American Association of Petroleum Geologists, 935–939 (2023).

Kim, J., and Kim, Y.: Spatiotemporal variation in upper crustal seismic anisotropy and VP/VS ratio in Groningen gas field, Netherlands: insights from shear wave splitting, Geophysical Journal International, 232(2), 1066–1082 (2023).

Kim, K.-H., Ree, J.-H., Kim, Y., Kim, S., Kang, S. Y., and Seo, W.: Assessing whether the 2017 M W 5.4 Pohang earthquake in South Korea was an induced event, Science, 360, 1007–1009 (2018).

Li, D., Huang, L., Li, Y., Zheng, Y., and Moore, J.: Seismic monitoring of EGS fracture stimulations at Utah FORGE (part 1): Time-lapse variations of b-values and shear-wave splitting rates of induced microearthquakes, Geothermics, 120, 103005 (2024).

Licciardi, A., Eken, T., Taymaz, T., Agostinetti, N. P., and Yolsal-Çevikbilen, S.: Seismic anisotropy in central North Anatolian Fault Zone and its implications on crustal deformation, Physics of the Earth and Planetary Interiors, 277, 99–112 (2018).

Moore, J., McLennan, J., Allis, R., Pankow, K., Simmons, S., Podgorney, R., Wannamaker, P., Bartley, J., Jones, C., and Rickard, W.: The Utah Frontier Observatory for Research in Geothermal Energy (FORGE): an international laboratory for enhanced geothermal system technology development, Proceedings, 44th Workshop on Geothermal Reservoir Engineering, Stanford University, 11–13 (2019).

Savage, M., Aoki, Y., Unglert, K., Ohkura, T., Umakoshi, K., Shimizu, H., Iguchi, M., Tameguri, T., Ohminato, T., and Mori, J.: Stress, strain rate and anisotropy in Kyushu, Japan, Earth and Planetary Science Letters, 439, 129–142 (2016).

Schultz, R., Skoumal, R. J., Brudzinski, R. M., Eaton, D., Baptie, B., and Ellsworth, W.: Hydraulic fracturing-induced seismicity, Reviews of Geophysics, 58, e2019RG000695 (2020).

Silver, P. G., and Chan, W. W.: Shear wave splitting and subcontinental mantle deformation, Journal of Geophysical Research: Solid Earth, 96, 16429–16454 (1991).

van Thienen-Visser, K., and Breunese, J.: Induced seismicity of the Groningen gas field: History and recent developments, The Leading Edge, 34, 664–671 (2015).

Xing, P., Wray, A., Velez-Arteaga, E., Finnila, A., Moore, J., Jones, C., Borchardt, E., and McLennan, J.: In-situ stresses and fractures inferred from image logs at Utah FORGE, Proceedings, 47th Workshop on Geothermal Reservoir Engineering, Stanford University, Stanford, California, USA, 7–9 (2022).